TELKOMNIKA, Vol.10, No.8, December 2012, pp. 2247~2252
e-ISSN: 2087-278X
accredited by DGHE (DIKTI), Decree No: 51/Dikti/Kep/2010

A SiC high-temperature Pressure Sensor Operating in Severe Condition

Haojie Lv[*1], Huiyong Yu[2], Guoqing Hu[3]
[1]School of Physics and Electronics, Henan University, Kaifeng, China
[2]Henan Mechanical and Electrical Engineering College, Xinxiang, China
[3]Dept. of Mechanical and Electrical Engineering, Xiamen University, Xiamen, China
*corresponding author, e-mail: haojielv@henu.edu.cn

Abstract

The traditional MEMS pressure sensor based on Silicon (Si) material has not been suitable for operating in severe condition such as high-temperature (>500℃). However, as an alternative material, Silicon Carbide (SiC) can be used in hash environment due to its unique properties. Hence this paper presents a touch mode capacitive pressure sensor with double-notches structure, which employs a special SiC-AlN-SiC sandwich structure to achieve high-accuracy pressure measurement in high-temperature environment. In order to get the relation of capacitance and external pressure, the large deflection theory is applied in simulation analysis of the diaphragm deformation. At the same time, the sandwich structure and technical process of the sensor are studied in the paper. The results showed that the sensor has excellent high-temperature performance due to application of SiC and AlN materials, and the sensor has higher sensitivity and longer linear range than traditional single-cavity structure. Consequently, the sensor can be applied to accuracy pressure measurement in high-temperature and harsh environment.

Keywords*: high-temperature, Silicon Carbide, pressure sensor, technical process*

1. Introduction

Microelectromechanical Systems (MEMS) allow interrelated device components to be integrated into comprehensive systems at very small scales which complete functions such as sensing and actuating. Therefore, MEMS were becoming an important area of technology combining material, mechanical, electrical, chemical, optical and fluids engineering disciplines, and have attracted considerable interest worldwide to lead to rapid developments especially over the past decade [1].

At present, the primary material used in MEMS remains Si because its microfabrication techniques are compatible with microelectronics processing. However, with an increasing demand for MEMS pressure sensors for harsh environment applications such as combustion processes, gas turbine control and oil industry, Silicon material has not been suitable for operating in severe conditions such as high temperatures (>500℃) due to creep under minimal load. As a result, Silicon Carbide (SiC) has long been recognized as an excellent candidate for microsensor applications in harsh environments due to its unique properties which include high hardness and wear resistivity, mechanical robustness, good thermal stability and chemical inertness. The development of SiC technology over the last few years has been quite dramatic with significant improvements in wafer growth technology, materials processing, electronic devices and, increasingly sensors [2-4].

In fact, as one of the third generation wide band gap semiconductor materials, SiC is only known IV-IV binary compound composed of Si and C. It exists in a large number of polytypes, which are distinguished by different crystal structures based on a variety of stacking sequence of Si-C sub-unit. There are over 100 of these SiC polytypes known, but the majority of research and application has concentrated on only three: 4H-, 6H- and 3C-SiC. Hexagonal 4H- and 6H-SiC are commercially available and their bulk substrates have been used to fabricate pressure sensors through bulk micromachining processes. Cubic 3C-SiC is the only SiC polytype that can be synthesized on Si substrates which enables deposition on large-area substrates. Therefore, in the last few years, 3C-SiC as the dominant polytype for MEMS applications has attracted most of the attention [5, 6].

Received September 27, 2012; Revised November 16, 2012; Accepted November 24, 2012

As one of the third generation wide band gap semiconductor materials, Aluminium Nitride (AlN) is used as electrical insulating ceramic in high-temperature applications. AlN is stable at high temperatures in inert atmospheres and melts at 2800℃ and is resistant to attack from mineral acids, strong alkalies and most molten salts. In addition, it is most important that AlN can be deposited in surface of 6H-SiC due to similar crystal structures [7]. Table1 shows the basic material properties of SiC semiconductor and AlN insulator in comparison to those of Si conventional semiconductor.

Table 1. Basic material properties of SiC and AlN in comparison to Si

Material	Si	3C-SiC	4H-SiC	6H-SiC	AlN
Forbidden band width (eV)	1.12	2.2	3.26	3.0	6.28
Lattice constant (Å)					
a	5.43	4.36	3.07	3.08	3.11
c			10.08	15.12	4.98
Thermal expansion coefficient (10^{-6}/K)	2.6	4.7	4.8	4.8	4.5
Density (g/cm^3)	2.33	3.21	3.21	3.20	3.26
Melting point (℃)	1690	3103	3103	3103	3273
Carrier mobility (cm^2/v•s)					
electron	1400	1000	900	400	-
hole	600	320	120	90	-
Breakdown electric field (MV/cm)	0.25	2.12	2.2	2.5	14
Dielectric constant	11.9	9.7	9.6	10	8.5
Thermal conductivity (W/cm•K)	1.5	4.9	4.9	4.9	3.0

It can be seen from Table 1 that AlN materials is dielectric, and SiC materials is a wide band-gap semiconductor. Hence consideration of candidate materials combination of MEMS, SiC-AlN is becoming a novel alternative to Si-SiO_2 as a dominant structure at present. Moreover, the SiC-AlN structure great promise for MEMS is also dictated by the good crystallochemical compatibility between SiC and A1N which manifests itself just as in the minute lattice mismatch (1%), in closely matching thermal expansion coefficient (those mismatch being within 8%). It is of great important for MEMS sensor that can reduce error and failure due to thermal expansion mismatch between the diaphragm and the substrate. In addition, both materials have excellent thermal conductivity as well as high Debye temperatures (TD_{SiC}=1430K; TD_{AlN}=950K) which are characteristics of their inherent perfect thermal resistance and low reactivity [8].

In order to achieve high-accuracy pressure measurement for high-temperature environment, a new Double-notches Touch Mode Capacitive Pressure Sensor (DTMCPS) based on SiC and AlN has been proposed in this paper. The sensor has a special SiC-AlN-SiC sandwich structure, which can not only withstand temperature as high as 500℃, but also greatly improve measuring performance than conventional capacitive pressure sensor due to working in touch mode. For example, the sensor has low temperature drift, neglectable stray capacity effect, large overload protection and high sensitivity in the near-linear operation range [9]. The special sandwich structure of the pressure sensor is shown in Figure 1. The basic device consists of an edge-clamped, circular SiC diaphragm suspended over a micromachined sealed vacuum layered cavity, isolation layer AlN between diaphragm and substrate SiC.

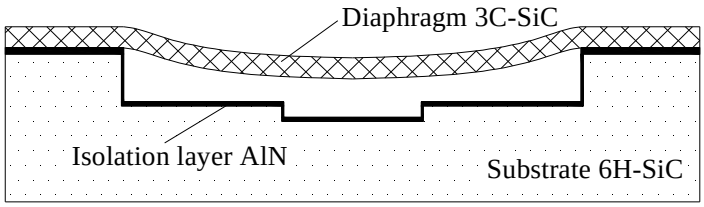

Figure 1. Cross-section view of material structure of pressure sensor

The diaphragm deflects toward the base of the cavity under the application of external pressure. When the external pressure increases to the Touch Point Pressure (TPP), the

diaphragm makes contact with the base of the sealed cavity causing a steep, nonlinear increase of capacitance with applied pressure. As the pressure is further increased into the touch mode, sufficient contact is made to linearize the capacitance output, as shown in Figure 2. The linear behavior in the touch mode gives the sensor a higher sensitivity than in the non-touch and saturation regions [10].

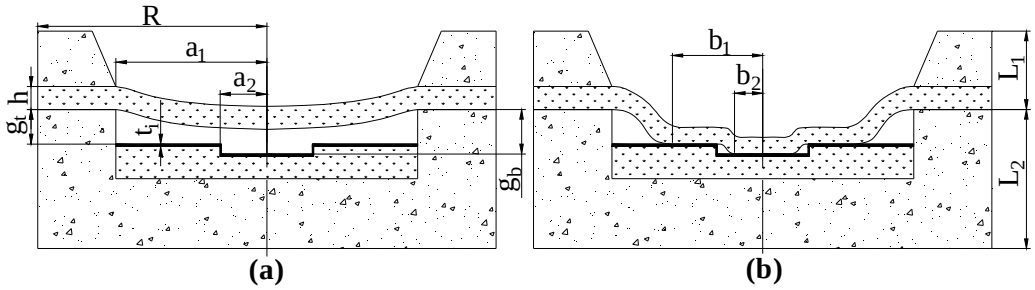

Figure 2. Cross-section view of operating state of the sensor (a-nomal mode, b-touch mode)

2. Research Method

In general, the deformation of the upper diaphragm under external pressure will lead to capacitance change of DTMCPS. For the circular diaphragm, the capacitance at equilibrium is expressed by [11]:

$$C=\int_0^{a_2}\frac{2\pi\varepsilon_0\varepsilon_a\varepsilon_i r_1 dr_1}{\varepsilon_a t_i+\varepsilon_i\left(g_b-w(r_1)\right)}+\int_{a_2}^{a_1}\frac{2\pi\varepsilon_0\varepsilon_a\varepsilon_i r_2 dr_2}{\varepsilon_a t_i+\varepsilon_i\left(g_t-w(r_2)\right)} \tag{1}$$

where C is capacitance; ε_0 is permittivity in vacuum; ε_a, ε_i are relative permittivity of air and insulation layer material, respectively; t_i is the thickness of the insulation layer; g_t, g_b are initial gap of the upper and lower cave, respectively; a_1, a_2 are radius of the upper and lower cave in bottom electrode, respectively; $w(r_1)$, $w(r_2)$ are the deflection of upper electrode diaphragm on region of 0 to a_2 and a_2 to a_1, respectively.

It can be seen from Equation (1) that the deflection of diaphragm w plays a key role during solving capacitance C. When external pressure is applied on the diaphragm of the sensor, the stresses caused by pressure will result in deformation of the diaphragm. For circular diaphragm, the general equation relating the large deflection of a diaphragm, with residual stress, in normal operation region can be described by [12]:

$$\begin{aligned}&\frac{d^4F}{dr^4}+\frac{2}{r}\frac{d^3F}{dr^3}-\frac{1}{r^2}\frac{d^2F}{dr^2}+\frac{1}{r^3}\frac{dF}{dr}=-F\left[\frac{\partial^2 w}{\partial r^2}\left(\frac{1}{r}\frac{\partial w}{\partial r}+\frac{1}{r^2}\frac{\partial^2 w}{\partial\theta^2}\right)-\frac{\partial}{\partial r}\left(\frac{1}{r}\frac{\partial w}{\partial\theta}\right)\frac{\partial}{\partial r}\left(\frac{1}{r}\frac{\partial w}{\partial\theta}\right)\right]\\&\frac{d^4w}{dr^4}+\frac{2}{r}\frac{d^3w}{dr^3}-\frac{1}{r^2}\frac{d^2w}{dr^2}+\frac{1}{r^3}\frac{dw}{dr}=\\&\frac{h}{D}\left[\frac{\partial^2 w}{\partial r^2}\left(\frac{1}{r}\frac{\partial F}{\partial r}+\frac{1}{r^2}\frac{\partial^2 F}{\partial\theta^2}\right)+\frac{\partial^2 F}{\partial r^2}\left(\frac{1}{r}\frac{\partial w}{\partial r}+\frac{1}{r^2}\frac{\partial^2 w}{\partial\theta^2}\right)-2\frac{\partial}{\partial r}\left(\frac{1}{r}\frac{\partial F}{\partial\theta}\right)\frac{\partial}{\partial r}\left(\frac{1}{r}\frac{\partial w}{\partial\theta}\right)\right]+\frac{q}{D}\end{aligned} \tag{2}$$

where w is deflection of diaphragm; F is a stress function which is related to the deflection of the diaphragm; θ is polar angle; $D=Eh^3/12(1-v^2)$ is flexural rigidity, E is Young's modulus, v is Poisson's ratio, h is thickness of diaphragm; q is pressure load.

As excellent Finite Element Analysis (FEA) software, ANSYS can be used to simulate the diaphragm deformation of touch mode pressure sensor, because this software can not only accurately model large displacement but also effectively simulate contact problem. Axis symmetry method is applied in FEA to reduce computing time and EPROM due to the diaphragm as studying object is circular. In addition, it is necessary to define two groups of contact pair as FEA due to two notches in substrate. By nonlinear ANSYS computing, the

deflection and stress at each node can be simulated when a set of sensor structure parameters are assumed: a_1=150μm, a_2=40μm, h=2μm, g_t=2.46μm, g_b=2.66μm and t_i=0.2μm. Consequently, the displacement and von mises stress of the sensor in touch mode can be attained after ANSYS postprocessor, as shown in Figure 2 and Figure 3, respectively.

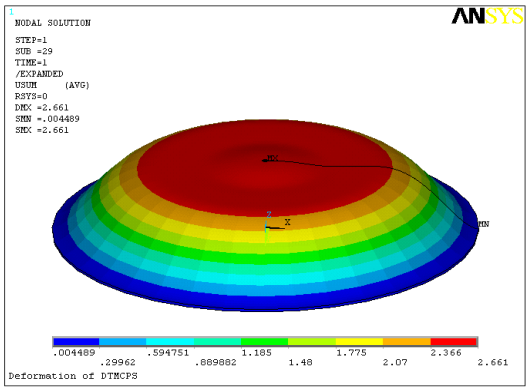

Figure 3. Displacement of diaphragm under 2MPa

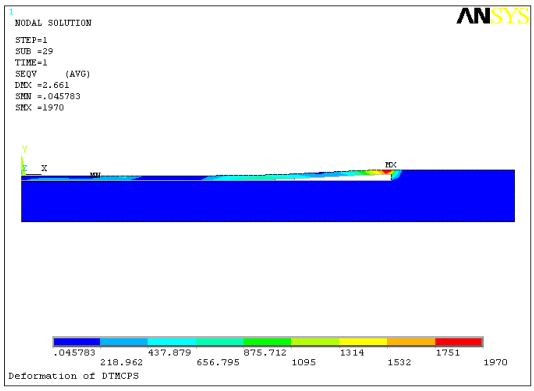

Figure 4. Von mises stress of the sensor under 2MPa

After using electric field FEA, the capacitance of the sensor will be obtained. Along with external pressure increasing, the output capacitance will rise constantly.

3. Results and Analysis

3.1. Performance Analysis and Discussion

When the corresponding capacitance under different external pressure are simulated by ANSYS software, the fitting curve about the output capacitance-input pressure (C-P) will be described, as shown in Figure 5.

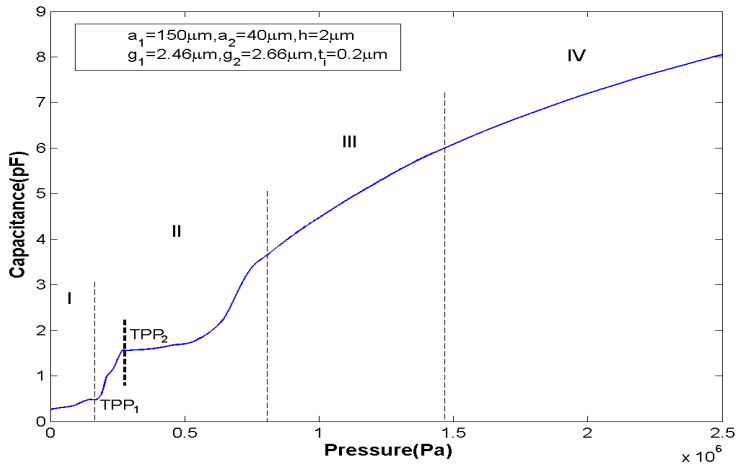

Figure 5. The C-P curve of double-notches structure pressure sensor

It can be seen from Figure 5 that the sensor has four operating regions: I normal, II transition, III linear (touch mode), IV saturation (touch mode). The linear region is main operating range of this sensor because the sensor has good linearity and sensitivity in the region. Obviously there are two TPPs because the diaphragm successively contacts with the two notches on substrate twice. In fact, that is main reason of the excellent performance of this sensor. In general, the higher sensitivity is obtained with lower TPP, yet the longer linear range

is obtained with higher TPP. Therefore two TPPs can meet the needs of sensitivity and linear range concurrently.

When g_t=g_b=2.66μm, double-notches structure of pressure sensor will become traditional single-cavity structure and both structure have same TPP. When g_t=g_b=5μm, the pressure sensor with double-notches and single-cavity structure will have same initial pressure in linear range. Consideration of double-notches structure pressure sensor, the C-P curve of traditional single-cavity pressure sensor for comparison will be described, as shown in Figure 6.

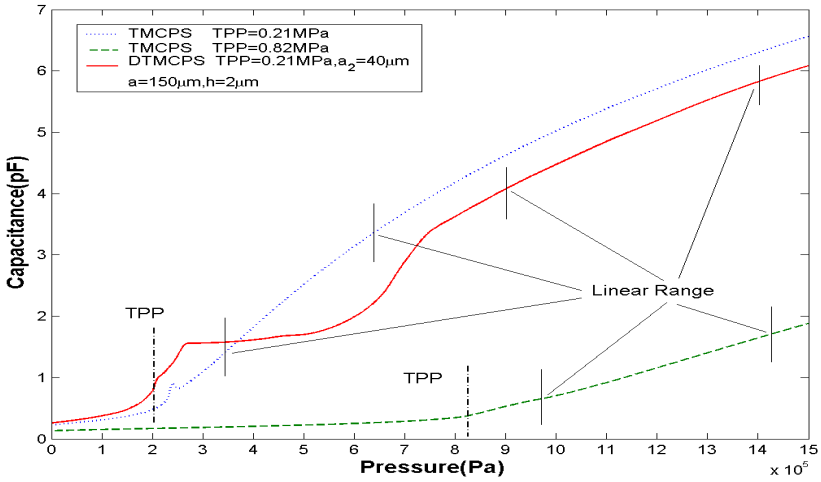

Figure 6. The C-P curves of double-notches and traditional single-cavity pressure sensor

It can be seen that the C-P curves after TPP are approximately linear, and the maximal nonlinearity is less than 3%. Assuming the TPP of double-notches pressure sensor is same to traditional single-cavity pressure sensor; linear pressure range of double-notches sensor will rise 1.6 times than traditional single-cavity sensor. However, when linear pressure range is same between the two sensors, the sensitivity of the former is greatly higher than the latter, so the output capacitance of double-notches sensor is about four times than the latter. The contrast description is shown in Table 2.

Table 2. The Performance of double-notches and single-cavity pressure sensor

Type of sensor	Design value of sensor (μm)								TPP (MPa)	Linear range (MPa)	Sensitivity (pF/MPa)	Non-linearity
	a_1	a_2	R	L_2	g_t	g_b	h	t_i				
Single-cavity	150	-	200	20	-	2.66	2	0.2	0.21	0.35-0.65	6.59	
Single-cavity	150	-	200	20	-	5.0	2	02	0.82	0.96-1.44	2.38	±3%
Double-notches	150	40	200	20	2.46	2.66	2	0.2	TPP_1=0.21 TPP_2=0.28	0.9-1.4	3.5	

3.2. Technical Process

In order to reduce stray capacitance, a reference capacitance is added in sensor structure, as shown in Figure 7. The technical process of the sensor can also be depicted from Figure 7. A 100mm diameter, single-crystal 6H-SiC wafer is used for the substrate. The double notches are made on the substrate through Reactive Ion Etching (RIE) technology. The capacitor bottom electrode on substrate is formed by aluminum diffusion on notches. A 0.2μm thick, low-stress AlN isolation film is deposited on full surface by Molecular Beam Epitaxy (MBE) technology. At the same time, a 3C-SiC film as the capacitor top electrode is deposited on single-crystal Si through Chemical Vapor Deposition (CVD) technology. The fusion bonding is used between 3C-SiC and AlN to form capacitor cavity [13]. Then Si layer on the back of 3C-

SiC is removed through using Tetramethyl ammonium hydroxide (TMAH). Finally, an AlN covering layer is deposited to seal and protect the sensor.

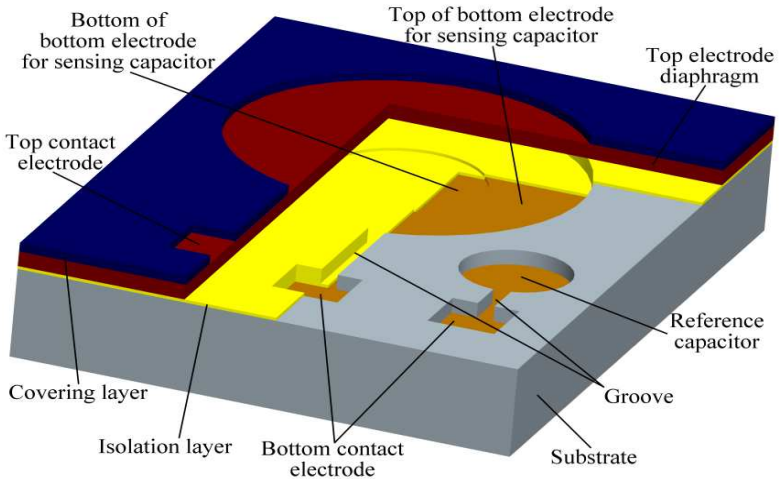

Figure 7. Three-dimensional structure profile of the sensor

4. Conclusion

In the paper, a pressure sensor with SiC-AlN-SiC sandwich structure is presented and analyzed. The sensor can work in harsh condition, especially 500℃ high-temperature environment. There are some reasons that SiC and AlN materials can resist high-temperature, and the technical process of the sensor is also beneficial to realize the goal of high-temperature resistance. In addition, the sensor can immensely improve the sensitivity and the linear range of traditional single-cavity sensor because of its double-notches structure. Hence this sensor will has good application prospect in harsh environment.

References

[1] Liudi Jiang, Rebecca Cheung. A Review of Silicon Carbide Development in MEMS Applications. *Int. J. Computational Materials Science and Surface Engineering*. 2009; 2: 225-240.
[2] G. L. Pearson, W. T. Read, jr, W. L. Feldman. Deformation and Fracture of Small Silicon Crystals. *Acta Metall*. 1957; 5: 181-191.
[3] Pasqualina M. Sarro. Silicon Carbide as a New MEMS Technology. *Sensors and Actuators*. 2000; 82: 210-218.
[4] N G Wright, A B Horsfall. SiC Sensors: a Review. *J. Phys. D: Applied Physics*. 2007; 40: 6345-6354.
[5] V Cimalla, J Pezoldt, O Ambacher. Group III Nitride and SiC Based MEMS and MENS: Materials properties, Technology and Applications. *J. Phys. D: Applied Physics*. 2007; 40: 6386-6434.
[6] Robert S. Okojie, Alexander A. Ned, Anthony D. Kurtz. Operation of α(6H)-SiC pressure sensor at 500 . *Sensor and Actuators A*. 1998; 66(3): 200-204.
[7] Shigehiro Nishino, J. Anthony Powell, Herbert A. Will. Production of Large-area Single-crystal Wafers of Cubic SiC for Semiconductor Devices. *Appl. Phys. Lett.*. 1983; 42(5): 460-462.
[8] Victor V. Luchinin, Andrey V. Korlyakov, Alexander A. Vasilev. *Silicon Carbide-Aluminium Nitride: a new high stability composition for MEMS*. Part of the Symposium on Design, Test and Microfabrication of MEMS and MOEMS. Paris. 1999; 782-791.
[9] H. J. Lv, Q. Guo, G. Q. Hu. *A touch mode capacitive pressure sensor with long linear range and high sensitivity*. 3rd IEEE International Conference of Nano/Micro Engineered and Molecular Systems. Sanya. 2008; 796-800.
[10] W. H. Ko, Q. Wang. Touch Mode Capacitive Pressure Sensors. *Sensors and Actuators A*. 1999; 75(3): 242-251.
[11] H. J. Lv, G. Q. Hu, W. Zou, C. Y. Wu, Y. F. Chen. Design and thermal analysis of high performance MEMS capacitive pressure sensor. *Optics and Precision Engineering*. 2010; 18(5): 1166-1174.
[12] S. Timoshenko, S. Woinowsky-Kreger. Theory of Plates and Shells, 2nd. New York: Mac Graw-Hill. 1959: 410-420.
[13] K. Nath, Alfred B. Anderson. Adhesion and bonding of polar and nonpolar SiC and AlN surfaces: tight-binding band theory. *Physical Review B*. 1989; 40(11): 7916-7922.